

Preparation and characterization of fibroin nanoparticles obtained from *Bombyx mori* L. Pilamo 1 cocoons

Gloria E. Guerrero Álvarez¹, Luz M. Baena*¹, Maria C. Giraldo¹

Edited by

Juan Carlos Salcedo-Reyes
salcedo.juan@javeriana.edu.co

1. Universidad Tecnológica de Pereira,
Faculty of Technology, School of
Chemistry, Oleochemistry Research
Group, Carrera 27 # 10-02 Barrio
Álamos, Pereira, Colombia, 660003

*lmbaena@utp.edu.co

Received: 01-03-2021

Accepted: 30-08-2022

Published online: 15-10-2022

Citation: Guerrero-Álvarez G, Baena
LM, Giraldo MC. Preparation and
characterization of fibroin nanoparticles
obtained from *Bombyx mori* L. Pilamo 1
cocoons, *Universitas Scientiarum*, 27(3):
275–290, 2022.
doi: 10.11144/Javeriana.SC273.pacof

Funding: n.a

Electronic supplementary material: n.a

Abstract

Silk fibroin (SF) is a biomacromolecule composed of proteins with properties, such as biocompatibility, biodegradability, and low immunogenicity. Thus, Silk fibroin nanoparticles (FNPs) overcome the disadvantages of non-degradable synthetic nanoparticles. We studied the structural and thermal properties of SF and FNPs from *Bombyx mori* L. cross-breed Pilamo I cocoons. Raw fibroin (RF) was obtained using a sodium Na₂CO₃ solution as part of an experimental design to improve extraction, and FNPs were obtained by denaturing RF with a ternary solution of CaCl₂:H₂O:CH₃CH₂OH, followed by precipitation using an anti-solvent method with propanol. Pilamo I cocoon, RF, and FNPs were characterized using Fourier-transform infrared spectroscopy (FTIR), scanning electron microscopy (SEM), and elemental chemical analysis of energy dispersive X-rays (EDS). The Light Scattering (DLS) and the thermal properties of RF and FNPs were studied by thermogravimetric analysis (TGA) and differential scanning calorimetry (DSC). The FTIR results showed that sericin-free raw fibroin was obtained, and the SEM results showed that the nanometer-sized particles had a globular structure and apparent porosity. The differences in the enthalpy of the crystallization peaks in the DSC and TGA curves showed that the FNPs had higher thermal stability than RF fibers. This result furthers the development of alternative materials as vehicles of active compounds from natural extracts.

Keywords: fibroin; nanoparticles; FTIR; SEM; thermogravimetric analysis



1. Introduction

Nanoparticles can serve as vehicles for active compounds (Faraji and Sepehri, 2018; Wenk *et al.*, 2011; Xu *et al.*, 2019) because of their biodegradability and controlled release rate capability (Lozano *et al.*, 2017). Natural polymers, such as proteins (Zhao *et al.*, 2015), have been used to produce nanoparticles. Silk fibroin (SF) is a polymeric biomaterial that exhibits unique and desirable structural properties, such as self-assembly, mechanical strength, processing flexibility, biodegradability, and biocompatibility (Koh *et al.*, 2015; Liu *et al.*, 2015; Lozano *et al.*, 2017).

Although SF has been used for thousands of years in the textile industry (Koh *et al.*, 2015), biotechnological improvements to this material have extended its use to generate scaffolds, films, hydrogels, and nanoparticles for several applications (Kim *et al.*, 2016; Niu *et al.*, 2019; Tudora *et al.*, 2013; Wu *et al.*, 2013; Yadav and Kumar, 2014). Fibroin is present in the cocoons of different *Bombyx mori* (the domestic silk moth) breeds, which typically grow and produce silk worldwide in a standardized climacteric manner (Cifuentes, 1999). However, the obtained fibroin varies in structure and physical-chemical properties (Jaramillo *et al.*, 2017; Koh *et al.*, 2015).



The Technological University of Pereira, in Colombia, houses a silkworm germplasm bank where the Pilamo I cross-breed was developed and adapted to local climatic conditions (Cifuentes, 1999). Pilamo I outperforms pure breeds in its resistance to diseases and unfavorable environments, so breeding occurs throughout the year. Cocoon features, the length and caliber of the filament, and the number of eggs per female in Pilamo I are also superior to those of pure breeds (Cifuentes, 1999).

This bank supplies national and international silk producers with mulberry seeds and Pilamo I *Bombyx mori* eggs (Cifuentes, 1999). However, the current local demand for silk has decreased, threatening the sustainability of industrial sericulture in the region. Therefore, we face the challenge of fully exploiting sericulture products and by-products for purposes beyond silk production and exploring the development of inputs for the industry. Moreover, this represents an opportunity for the University to grow research in related areas and creates a window to commercializing products and services.

Considering the potential of this biomaterial, the present study was conducted to obtain and characterize fibroin and its corresponding nanoparticles, which may serve as a vehicle for the nanoencapsulation of active compounds from different natural extracts.

2. Materials and methods

2.1. Materials

Bombyx mori L. Pilamo I cross-breed silkworm cocoons were supplied by the Asociación de Mujeres Mundo Café y Seda (Women's Association for World Coffee and Silk) in the municipality of Guatica, Risaralda, Colombia. The fluff from the cocoons was removed, and the pupae were inactivated following established methodologies. The pupae were then manually removed from the cocoons, and the cocoons were stored at room temperature in a cool, dark place. All analytical grade chemicals employed were purchased from Sigma Aldrich S.A.

2.2. Raw fibroin obtention

Pilamo I cocoons were milled with a blade mill (IKA MF 10 basic) to a thickness of approximately 2 mm. To separate the raw fibroin from the sericin, the milled cocoons were subjected to an alkaline digestion by immersing them in a Na_2CO_3 solution, with magnetic stirring at 600 rpm at a constant boiling temperature. This alkaline digestion step was carried out with different Na_2CO_3 concentrations (0.5 M and 1 M) and agitation times (30 min and 90 min), as shown in Table 1 (Daithankar *et al.*, 2005; Lozano *et al.*, 2017).

2.3. Liquid silk fibroin preparation

Raw fibroin was dissolved in a ternary solution of $\text{CaCl}_2:\text{CH}_3\text{CH}_2\text{OH}:\text{H}_2\text{O}$ (1:2:8) according to the protocol established by Gregory *et al.* (2019), at a constant temperature and agitation speed for 180 min. Dialysis was then performed using a semipermeable cellulose membrane (Spectra/Por Molecular porous 1000 Da) for 72 h using distilled water at 8 °C and a constant agitation speed (Yadav and Kumar, 2014).

2.4. Obtention of silk fibroin nanoparticles

Silk fibroin nanoparticles were obtained by an anti-solvent method with propanol, modifying the methods by (Labconco Freezone) (Lozano *et al.*, 2017; Montalbán, 2016; Yadav and Kumar, 2014). To get the nanoparticles a freshly prepared aqueous silk fibroin solution at 1000 mg L^{-1} by weight was slowly dropped into propanol with constant stirring. After a few drops, a white suspension appeared, which was stirred for 2 h. The particle suspension was recovered by centrifugation at 4000 rpm for 15 min at room temperature.

2.5. Characterization of raw fibroin and silk fibroin nanoparticles

The physical and chemical properties of the obtained Pilamo I raw fibroin and fibroin nanoparticles, along with silk worm cocoons, for comparisons sake, were studied with set of techniques as follows.

An infrared analysis (IR-TF) was performed in an Agilent Cary 630 equipment. The infrared spectra of crude fibroin and fibroin nanoparticles were then analyzed according to standard protocols (Lozano *et al.*, 2017; Montalbán, 2016; Yadav and Kumar, 2014).

Raw fibroin and fibroin nanoparticles were subjected to Thermogravimetric Analysis (TGA) and Differential Scanning Calorimetry (DSC) assays. Both assays were carried out in a Thermo brand TGA-DSC equipment with a heat increase of $10 \text{ }^\circ\text{C min}^{-1}$ and in a nitrogen-atmosphere following Loganathan *et al.* (2017).

Scanning Electron Microscopy (SEM) images were taken on raw fibroin and fibroin nanoparticles samples with an SEM FEI Quanta-FEG 250 equipment with Gatan Chroma CL to reveal morphological differentiation, phase identification, and particle dispersion in nanometric and micrometric scales (Lozano *et al.*, 2017; Montalbán, 2016; Yadav and Kumar, 2014).

An energy-dispersive X-ray spectroscopy (EDS) analysis was conducted to characterize the microstructure of fibroin nanoparticles. Furthermore, we used Dynamic Light Scattering (DLS) in a Malvern Zetasizer Nano ZS instrument, to assess the mean diameter of fibroin nanoparticles along with their size distribution and Zeta potential. All measurements were made in propanol at $25 \text{ }^\circ\text{C}$. The Z-average and polydispersity values were calculated with the software provided by the manufacturer, and to obtain the nanoparticles' mean diameter, values were calculated from duplicate measurements.

2.6. Statistical analysis

All results were expressed as the mean \pm SD. An analysis of variance (ANOVA) was performed, and statistically significant differences were recognized at $p < 0.05$. All of the results were processed in Statistica 10 (version 10.0228.2, Statsoft Inc. 2011, Australia).

3. Results and discussion

In this study, the average raw fibroin content of the assessed Pilamo I cocoons was of $(69.7 \pm 3.6) \%$, close to raw fibroin values of 70 % and 85 % in silkworm cocoon assessments conducted by other authors (Montalbán, 2016). The raw fibroin content results, showed in Table 1, were not significantly different ($p > 0.05$) with the four tested extraction protocols with varying agitation time and Na_2CO_3 concentration.

Table 1. Fibroin content in Pilamo I silkworm cocoons according to varying extraction conditions. Results are presented as mean \pm SD. Different superscript letters, *a* and *b*, indicate significant differences

Trials	Fibroin obtained (%)
1	86.80 \pm 0.34 ^a
2	94.23 \pm 7.82 ^a
3	71.07 \pm 2.52 ^a
4	76.00 \pm 6.56 ^a
5	72.10 \pm 1.74 ^a

Therefore, to determine the best digestion conditions, fibroin content data were plotted in a histogram (Figure 1), revealing that a fibroin output range of 65 % and 75 % was most frequent when extractions were carried out with 0.75 M Na₂CO₃ and a stirring time of 70 min. These results are comparable to reports from other silk cocoon fibroin content studies, in which the most common output range was 72 %-82 % (Qu *et al.*, 2014; Zhang *et al.*, 2007).

Since fibroin and sericin are two main proteins in silk, and our previous, unpublished, Pilamo I silk cocoon composition assessment revealed that its sericin content is approximately 20 %, we can be confident that the digestion implemented to obtain fibroin is adequate. However, further studies are required to reduce the concentration of carbonate employed in the process.

3.1. Raw fibroin and fibroin nanoparticle characterization

3.1.1. Fourier transform infrared (FTIR) analysis

The infrared spectra of the assessed Pilamo I silkworm cocoons, their raw fibroin, and their fibroin nanoparticles are shown in Figure 2.

The FTIR spectrum of Pilamo I cocoons revealed the following features (Figure 2a). A band at 3222.7 cm⁻¹ is attributed to the vibrational stretching of OH⁻ groups that are associated with hydrogen bonds in the hydrophilic residues of the sericin side chain; A band at 2877.8 cm⁻¹,

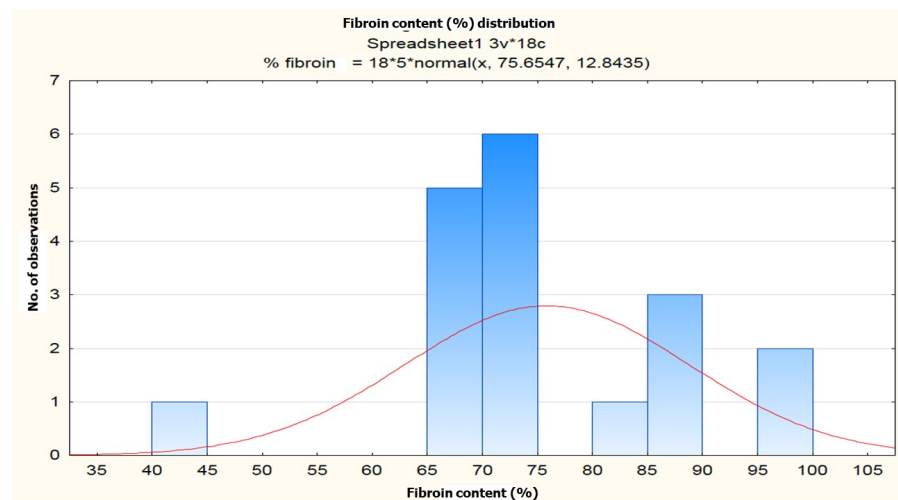


Figure 1. Histogram of fibroin percentage obtained by varying concentration and stirring time.

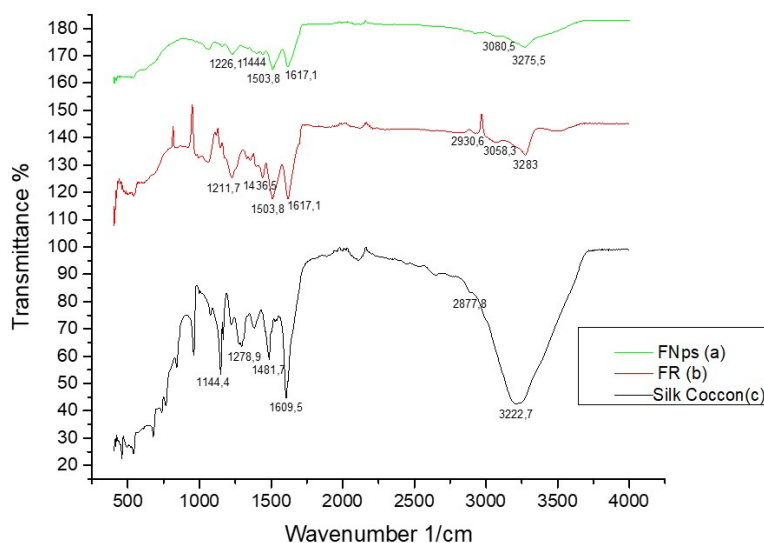


Figure 2. Full infrared spectra including peak labels of: (a) fibroin nanoparticles (FNps); (b) raw fibroin (RF); and (c) Pilamo I cocoons.

associated with the asymmetric stretching of C–H; a band at 1609.5 cm^{-1} , associated with the vibrational stretching of the C=O group of fibroin conformations of parallel β -sheet structures (Xie *et al.*, 2015; Zhang *et al.*, 2007); a band at 1228 cm^{-1} corresponding to a tertiary amino group; a band at 1503.8 cm^{-1} , that could be attributed to a symmetrical N–H bending mode and the C–N vibrational stretching mode of a secondary amide; and bands at 1481.7 cm^{-1} and 1400 cm^{-1} , which are attributed to OH^- groups for side chains containing sericin and threonine (Chelazzi *et al.*, 2020; Chen *et al.*, 2012; Koperska *et al.*, 2014).

The raw fibroin FTIR spectrum (Figure 2b) exhibited the following characteristics: a band at 3283 cm^{-1} , attributed to N–H vibrational stretching; a band at 1617.1 cm^{-1} , attributed to C=O vibrational stretching; a band at 1503.8 cm^{-1} , likely corresponding to the symmetric flexion movement of the N–H bond and the C–N vibrational stretching mode of a secondary amide; a band at 1436.9 cm^{-1} , attributed the symmetric flexion of CH_3 , and a band at 1069 cm^{-1} , related to the presence of a tertiary amino group whose signal results from a symmetrical N–H flexion mode, a C=O stretching mode, and stretching modes of the peptide bond (Xie *et al.*, 2015; Zhang *et al.*, 2007; Zhao *et al.*, 2015).

The comparison of the two abovementioned infrared spectra revealed that many of the signals coincide with each other and that the most significant protein functional groups, such as N–H, N–H₂, N–H₃ and C=O, were present in both materials. However, the fibroin spectrum differs from the silkworm cocoon spectrum by the absence of an OH^- signal at 3273 cm^{-1} . This signal indicates the presence of sericin, which must have been separated out from the proteins that make up the silkworm cocoon (Xie *et al.*, 2015; Zhang *et al.*, 2007; Zhao *et al.*, 2015).

The infrared spectrum of the obtained fibroin nanoparticles, shown in Figure 2c, resembles that of raw fibroin in terms of vibration band assignments for the amide region of the spectrum; however, the intensity of the signal decreases, indicating that the protein has been altered by the

denaturation, precipitation, and regeneration processes to which it was subjected. Furthermore, this profile is characteristic of crystalline and insoluble silk (having a β -sheet structure), as other groups have reported (Lozano *et al.*, 2017).

3.1.2. Raw fibroin and fibroin nanoparticle thermal properties

Raw fibroin and its nanoparticle's TGA results are presented in Figure 3. Raw fibroin's thermogram (Figure 3a) revealed a weight loss in several phases. Between temperatures of 30 °C and 115 °C raw fibroin weight went down to 28 % of its initial weight due to water evaporation, between 227 °C and 297 °C the observed fibroin weight loss was attributed denaturation, resulting in the loss of its β -sheet structure, associated with the rupture of the side groups of amino acid residue chains and peptides. The temperatures of raw fibroin denaturation and water loss at different concentrations and times revealed the connection between these two processes, despite fibroin decomposition (Ma *et al.*, 2018; Zhao *et al.*, 2015). Finally, fibroin nanoparticles had higher thermal stability than raw fibroin, as implied by the observed minimal weight loss as temperature increased (Figure 3b). However, the shape of these curves may differ depending on initial sample weight and surface oxidation reactions taking place in a reaction atmosphere (Loganathan *et al.*, 2017).

Raw fibroin and fibroin nanoparticle endotherms (Figure 4) can be used to determine their glass transition temperature (T_g), as well as their crystallization and melting temperatures (T_c and T_m). Glass transition in the Raw fibroin endotherm occurs at 52 °C-157 °C, where amorphous regions briefly increase before a crystallization event at 283 °C-325 °C, and a structural relaxation occurs facilitating β -sheet constitution (Loganathan *et al.*, 2017; Zhao *et al.*, 2015). In other studies, glass transitions have occurred between 175 °C and 179 °C, and crystallization between 212 °C and 220 °C. A glass transition between 52 °C-179 °C was not observed in the DCS analysis of fibroin nanoparticles; however, the structural relaxation transition that facilitates the β -sheet re-arrangement was detected (Zhang *et al.*, 2007). This result indicates that the decrease in raw

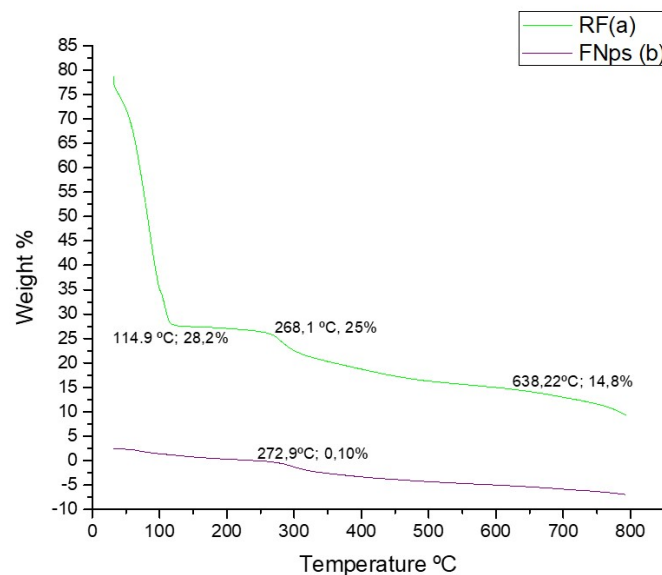


Figure 3. Thermogravimetric Analysis of: fibroin nanoparticles FNps (a) and Raw Fibroin RF (b) from Pilamo I cocoons.

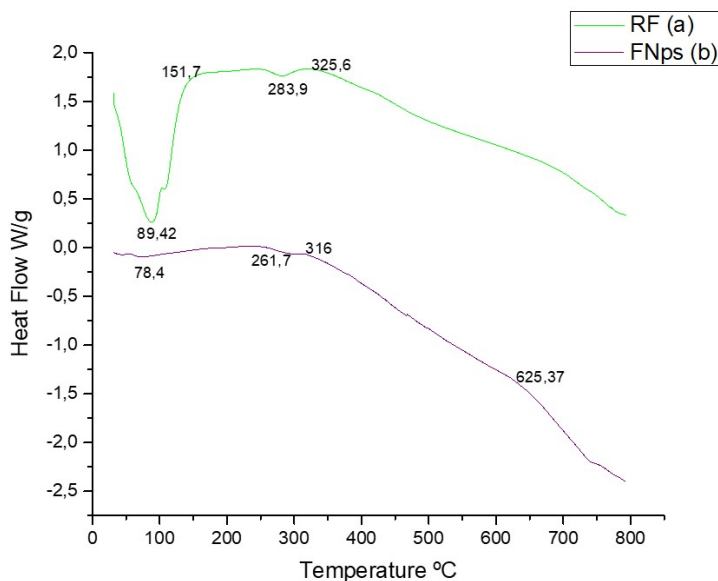


Figure 4. DSC analyses thermogram of fibroin nanoparticles FNps (a) and Raw Fibroin RF (b) from Pilamo I cocoons.

fibroin's thermal stability is apparently related to the breakdown of amide bonds and the non-oriented arrangement of the β -sheet (Zhang *et al.*, 2007). Therefore, fibroin nanoparticles could be a suitable vehicle for the transport and preservation of compounds sensitive to atmospheric conditions

3.1.3. SEM analysis for raw fibroin and fibroin nanoparticles

Figure 5 and Figure 6 are SEM micrographs raw fibroin and fibroin nanoparticles, respectively. SEM revealed raw fibroin's fibrous structure with an average diameter of $(8.832 \pm 1.390) \mu\text{m}$ for $p > 0.05$, and fibers intertwined with no apparent porosity, which is in agreement with results reported in other studies (Mollahosseini *et al.*, 2019; Montalbán, 2016; Zhao *et al.*, 2015). fibroin nanoparticles had an average diameter of $(486.16 \pm 72.95) \text{nm}$ ($p > 0.05$) and tended to agglomerate due to the unevenness of the cocoon's silk fibers and abrasive effect of the Na_2CO_3 treatment, decreasing fiber quality. Nanoparticles typically have sizes in the 0.1 nm-100 nm range, suitable for multiple nanotechnological applications; however, studies have shown that the uptake and release of compounds by nanoparticles is negatively related to particle size (?). In this study, we used a high-molecular-weight macromolecule that generates particles larger than 100 nm in size while remaining functional (Montalbán, 2016). In addition, physical and chemical processes, such as the addition of coagulation reagents, aeration, and coagulation at the protein's isoelectric point, alter particle sizes (Zhang *et al.*, 2007). Finally, other studies have reported that a high protein concentration causes marked supersaturation, which leads to rapid nucleation and the subsequent production of small particles with a narrow size distribution. Nevertheless, the particles obtained in this study are composed of a material that can be used for the nanoencapsulation of active compounds present in natural extracts.

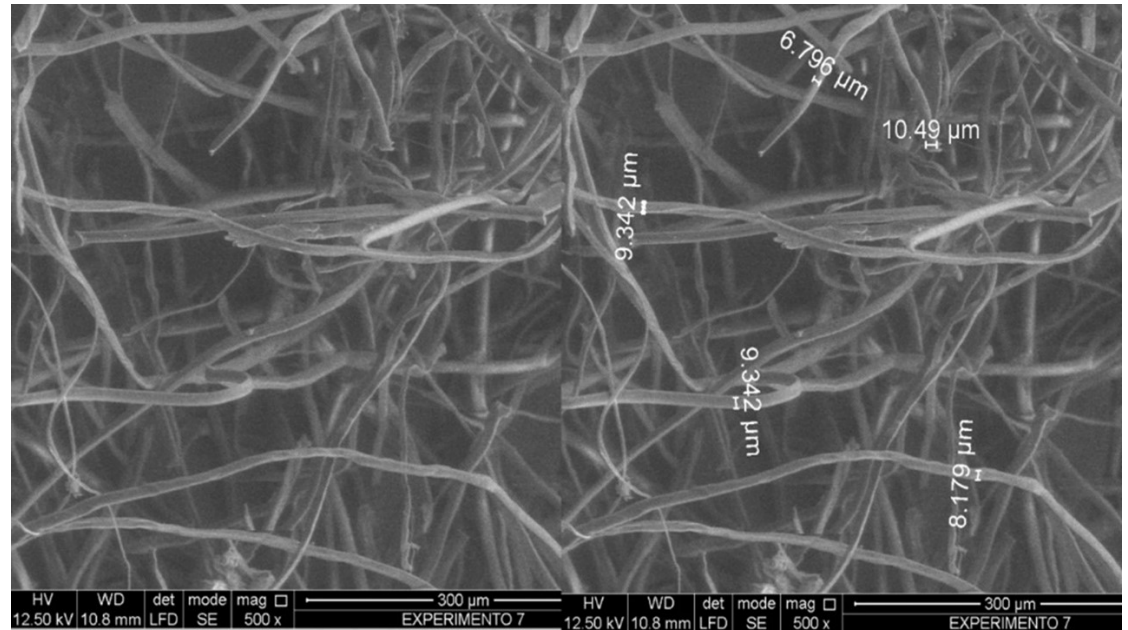


Figure 5. SEM micrograph of Raw Fibroin (RF).

3.1.4. Elemental chemical properties of fibroin nanoparticles

The elemental chemical analysis of the fibroin nanoparticles obtained was performed using a points of interest analysis, through profiles or maps. Figure 7 shows the microscopic magnification of fibroin nanoparticles, in which carbon was abundant (46.07 %), followed by nitrogen 21.43 %, and oxygen 21.81 %. This profile coincides with the chemical structure of the fibroin molecule, which

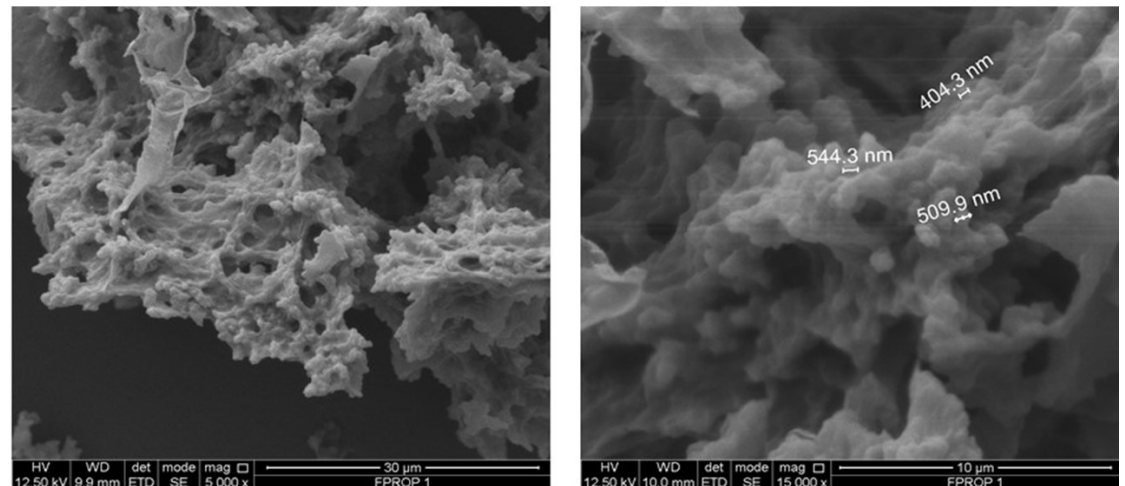


Figure 6. SEM micrographs of Fibroin Nanoparticles (FNPs) from Pilamo I cocoons, obtained using a propanol anti-solvent.

is chiefly composed of amino acids such as glycine, serine, and alanine. The least represented elements in the sample were iron, chlorine, and calcium, which may be present due to an incomplete dialysis process in the protein regeneration process. The absence of sulfur reveals that the protein's disulfide bonds have disappeared, indicating a reestablishment of its β -sheet structure. This has been observed by other X-ray diffraction analyses on fibroin nanoparticles with completely crystalline forms.

The stability of the suspended particles was tested in 2-propanol using dynamic light scattering (DLS). Empty fibroin nanoparticles showed a Z-average diameter of (295.35 ± 40.82) nm (PDI = 0.329), as shown in Figure 8. The profile revealed substantial particle polydispersity. Nevertheless; the particle sizes fit the concept of nanoparticles and complement the analyses obtained by SEM, where due to agglomeration it was difficult to determine the exact particle size value. The analysis values are almost identical to those previously described in the corresponding literature (Montalbán, 2016).

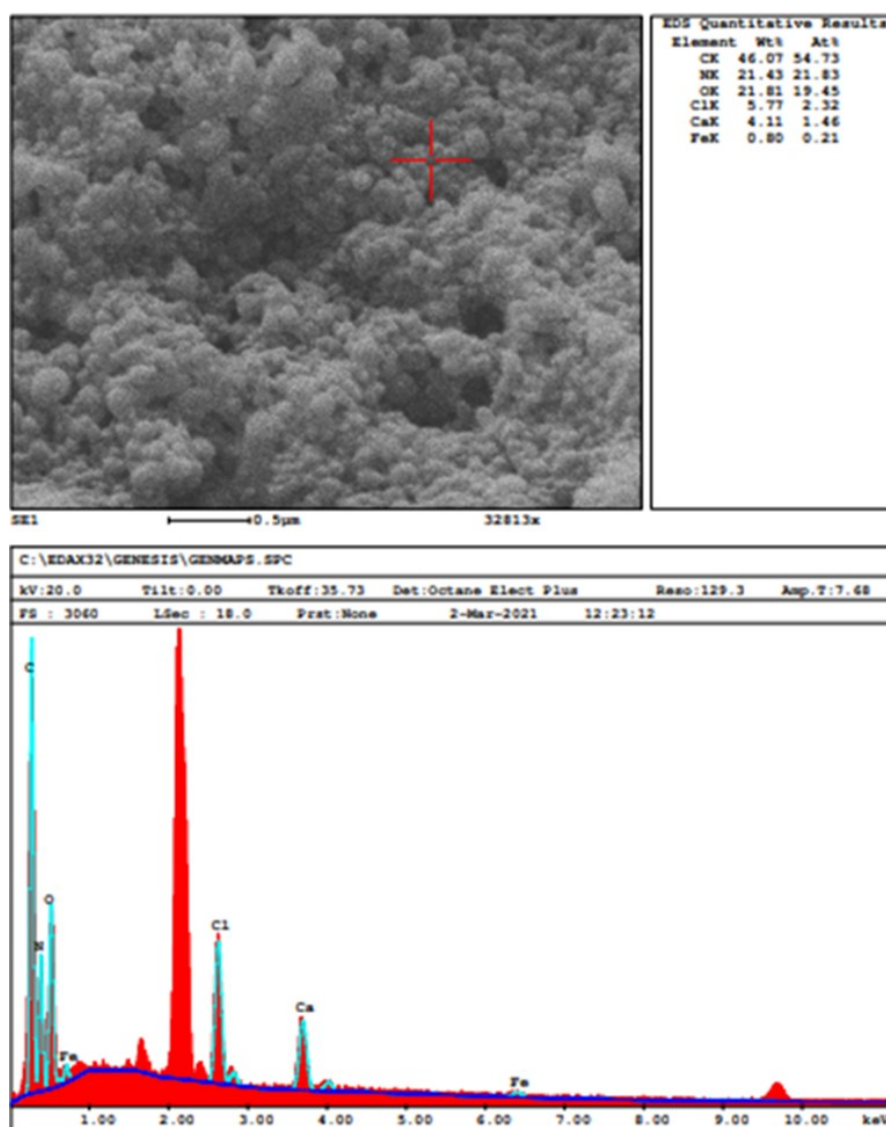


Figure 7. Elemental composition profile and Energy Dispersive X-ray Spectrum (EDS) of fibroin nanoparticles from *Bombyx mori* L. Pilamo 1 cocoons.

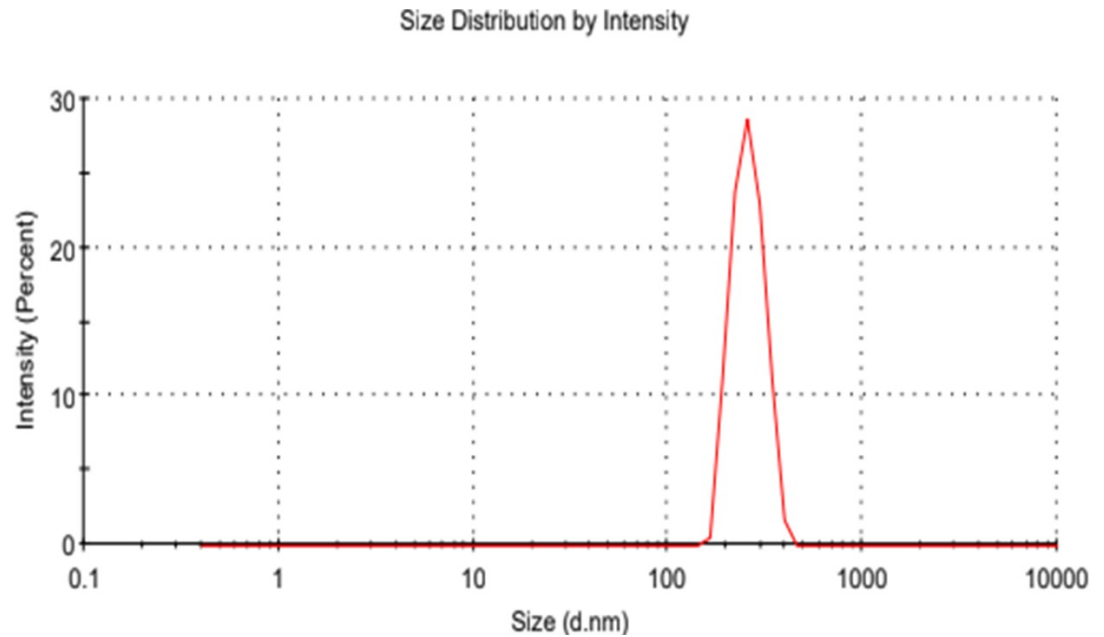


Figure 8. Size distributions of fibroin nanoparticles from Pilamo I cocoons.

4. Conclusions

We implemented a protocol for the obtention of fibroin from the cocoon of Pilamo I silkworms. Optimal fibroin extractions were obtained using Na_2CO_3 0.75 M and a stirring time of 70 min. The FT-IR spectra of the extracted fibroin confirmed the absence of sericine, and the microscopic SEM analysis revealed a fibrous material with no other adhering materials. Finally, it was possible to obtain fibroin nanoparticles in spherical shape, with diameters between 400 nm and 540 nm using the antisolvent method with 2-propanol. Nevertheless; in the DLS analysis, the particle size is between 263.4 nm and 327.3 nm, revealing a great dispersity. This may be an attribute of the material studied.

In general, the results of this study confirm the potential of Pilamo I *Bombyx mori* L, as a source of fibroin nanoparticles, furthering the development of alternative materials that can serve as transport media for active compounds of natural extracts.

5. Conflicts of interest

The authors declare no conflict of interest.

6. Acknowledgements

This work was funded through a grant by the Vice Presidency for Research, Innovation, and Extension at Universidad Tecnológica de Pereira.

References

- Chelazzi D, Badillo D, Giorgi R, Cincinelli P, Cincinelli A, Banglioni P. Self-Regenerated Silk Fibroin with Controlled Crystallinity for the Reinforcement of Silk, *Journal of Colloid and Interface Science*, 576: 230–40, 2020.
doi: 10.1016/j.jcis.2020.04.114
- Cifuentes C. *Manual Técnico de Sericultura*, 1st ed. Fondo editorial de Risaralda, Pereira, 1999.
- Daithankar V, Padamwar M, Pisal S, Mahadik K. Moisturizing Efficiency of Silk Protein Hydrolysate: Silk Fibroin, *Indian Journal of Biotechnology*, 4(1): 115–21, 2005.
- Chen, Porter D, Vollrath F. Silk Cocoon (*Bombyx Mori*): Multi-Layer Structure and Mechanical Properties, *Acta Biomaterialia*, 8: 2620–27, 2012.
doi: 10.1016/j.actbio.2012.03.043
- Faraji J, Sepehri A. Titanium Dioxide Nanoparticles and Sodium Nitroprusside Alleviate the Adverse Effects of Cadmium Stress on Germination and Seedling Growth of Wheat (*Triticum Aestivum L.*). *Universitas Scientiarum*, 23(1): 61–87, 2018.
doi: 10.11144/Javeriana.SC23-1.tdna
- Gregory D, Kumar P, Jimenez A, Zhang Y, Ebbens S, Zhao X. Reactive Inkjet Printing and Propulsion Analysis of Silk-Based Self-Propelled Micro-Stirrers, *Journal of Visualized Experiments*, (146): 1–10, 2019.
doi: 10.3791/59030
- Mohammad H, Ramkumar S. Functionalized Nanofibers for Advanced Applications, *Indian Journal of Fibre and Textile Research*, 31(1): 41–51, 2006.
- Jaramillo N, Álvarez C, Restrepo A. Structural and Thermal Properties of Silk Fibroin Films Obtained from Cocoon and Waste Silk Fibers as Raw Materials, *Procedia Engineering*, 200: 384–88, 2017.
doi: 10.1016/j.proeng.2017.07.054
- Kim H, Song D, Kim M, Ryu S, Um I, Ki C, Park Y. Effect of Silk Fibroin Molecular Weight on Physical Property of Silk Hydrogel, *Polymer*, 90: 26–33, 2016.
doi: 10.1016/j.polymer.2016.02.054
- Koh L, Cheng Y, Teng C, Khin Y, Loh X, Tee S, Low M, Ye E, Yu H, Zhang Y, Han M. Structures, Mechanical Properties and Applications of Silk Fibroin Materials, *Progress in Polymer Science*, 46: 86–110, 2015.
doi: 10.1016/j.propolymsci.2015.02.001
- Koperska M, Pawcwnis D, Bagniuk M, Zaitz M, Missori M, Lojewski T, Lojewska J. Degradation Markers of Fibroin in Silk through Infrared Spectroscopy, *Polymer Degradation and Stability*, 105(1): 185–96, 2014.
doi: 10.1016/j.polymdegradstab.2014.04.008
- Liu B, Song Y, Jin L, Wang Z, Pu D, Lin S, Zhou C, You H, Ma Y, Li Y, Sung P, Zhang Y. Silk Structure and Degradation, *Colloids and Surfaces B: Biointerfaces*, 131: 122–28, 2015.
doi: 10.1016/j.colsurfb.2015.04.040

- Loganathan S, Babu V, Mishra R, Pugazhenti G, Thomas S. Thermogravimetric Analysis for Characterization of Nanomaterials, *Thermal and Rheological Measurement Techniques for Nanomaterials Characterization*, 67–108, 2017.
doi: 10.1016/B978-0-323-46139-9.00004-9
- Lozano A, Correa H, Pérez M, Pagan A, Montalban M, Villora G, Cénis J. Silk Fibroin Nanoparticles: Efficient Vehicles for the Natural Antioxidant Quercetin, *International Journal of Pharmaceutics*, 518(1–2): 11–19, 2017.
doi: 10.1016/j.ijpharm.2016.12.046
- Ma D, Yansong W, Wenjie D. Silk Fibroin-Based Biomaterials for Musculoskeletal Tissue Engineering, *Materials Science and Engineering, C* 89(23): 456–69, 2018.
doi: 10.1016/j.msec.2018.04.062
- Mollahosseini H, Fashandi H, Khoddami Akbar, Zarrebini M, Nikukar H. Recycling of Waste Silk Fibers towards Silk Fibroin Fibers with Different Structures through Wet Spinning Technique, *Journal of Cleaner Production*, 236: 117653, 2019.
doi: 10.1016/j.jclepro.2019.117653
- Montalbán M. Propiedades de Líquidos Iónicos y Su Aplicación a La Síntesis de Nanopartículas, *Tesis Doctoral*, Universidad de Murcia, 2016.
<http://hdl.handle.net/10803/399283>
- Niu S, William G, Wu J, Zharing X, Zheng H, Li S, Zhu L. A Novel Chitosan-Based Nanomedicine for Multi-Drug Resistant Breast Cancer Therapy, *Chemical Engineering Journal*, 369: 134–49, 2019.
doi: 10.1016/j.cej.2019.02.201
- Qu J, Liu Y, Yu Y, Li J, Luo J, Li M. Silk Fibroin Nanoparticles Prepared by Electrospray as Controlled Release Carriers of Cisplatin, *Materials Science and Engineering, C* 44: 166–74, 2014.
doi: 10.1016/j.msec.2014.08.034
- Tudora M, Zaharia C, Stancu I, Vasile E, Truca R, Cincu C. Natural Silk Fibroin Micro- and Nanoparticles with Potential Uses in Drug Delivery Systems, *UPB Scientific Bulletin, Series B: Chemistry and Materials Science*, 75(1): 43–52, 2013.
https://www.scientificbulletin.upb.ro/rev_docs_arhiva/fullced_880511.pdf
- Wenk E, Merkle H, Meinel L. Silk Fibroin as a Vehicle for Drug Delivery Applications, *Journal of Controlled Release*, 150(2): 128–41, 2011.
doi: 10.1016/j.jconrel.2010.11.007
- Wu M, Zhu L, Zhou Z, Zhang Y. Coimmobilization of Naringinases on Silk Fibroin Nanoparticles and Its Application in Food Packaging, *Journal of Nanoparticles*, 1–5, 2013.
doi: 10.1155/2013/901401
- Xie M, Li Y, Zhao Z, Chen A, Li J, Hu J. Solubility Enhancement of Curcumin via Supercritical CO₂ Based Silk Fibroin Carrier, *Journal of Supercritical Fluids*, 103: 1–9, 2015.
doi: 10.1016/j.supflu.2015.04.021
- Xu Z, Shi L, Yang M, Zhu L. Preparation and Biomedical Applications of Silk Fibroin-Nanoparticles Composites with Enhanced Properties, A Review, *Materials Science and Engineering, C* 95: 302–11, 2019.
doi: 10.1016/j.msec.2018.11.010

- Yadav D, Kumar N. Nanonization of Curcumin by Antisolvent Precipitation: Process Development, Characterization, Freeze Drying and Stability Performance, *International Journal of Pharmaceutics*, 477(1–2): 564–77, 2014.
doi: 10.1016/j.ijpharm.2014.10.070
- Zhang Y, Shen W, Xiang R, Zhunge L, Gag W, Wang W. Formation of Silk Fibroin Nanoparticles in Water-Miscible Organic Solvent and Their Characterization, *Journal of Nanoparticle Research*, 9(5): 885–900, 2007.
doi: 10.1007/s11051-006-9162-x
- Zhao Z, Li Y, Xie M. Silk Fibroin-Based Nanoparticles for Drug Delivery, *International Journal of Molecular Sciences*, 16(3): 4880–4903, 2015.
doi: 10.3390/ijms16034880

Preparación y caracterización de nanopartículas de fibroína obtenida de capullos de *Bombyx mori* L. Pilamo I

Resumen: La fibroína de la seda (FS) es una biomacromolécula compuesta de proteínas con propiedades como biocompatibilidad, biodegradabilidad y baja inmunogenicidad. Por ello, las nanopartículas de SF (FNps) superan las desventajas de las nanopartículas sintéticas no biodegradables. En el presente trabajo, se estudiaron las propiedades estructurales y térmicas de la SF obtenida de capullos de Pilamo I, un cruce entre razas de *Bombyx mori* L. Se extrajo la fibroína cruda (RF) usando una solución de Na_2CO_3 siendo parte de un diseño experimental para optimizar la obtención de RF. Las FNps se prepararon por denaturación de la RF con una solución ternaria de $\text{CaCl}_2:\text{H}_2\text{O}:\text{CH}_3\text{CH}_2\text{OH}$, seguida de precipitación, usando un método anti-solvente con propanol. Los capullos de Pilamo I, la RF y las FNps se caracterizaron usando espectroscopía infrarroja con transformada de Fourier (FTIR), microscopía electrónica de barrido (SEM) y análisis químico estructural de energía dispersiva de rayos X (EDS). La dispersión de la luz (DLS), así como las propiedades térmicas de la RF y de los FNps se estudiaron por análisis termogravimétrico (TGA) y calorimetría diferencial de barrido (DSC). Los resultados de la FTIR mostraron que la fibroína obtenida estaba libre de sericina y los resultados de SEM mostraron que se produjeron partículas nanométricas con una estructura globular y porosidad aparente. Las diferencias en la entalpía de los picos de cristalización en las curvas de la DSC y el TGA mostraron que los FNps tenían mayor estabilidad térmica que las fibras de RF. Este resultado constituye un avance en el desarrollo de materiales alternativos que puedan servir como vehículos para transportar compuestos activos de extractos naturales.

Palabras Clave: fibroína, nanopartículas, FTIR, SEM, análisis termogravimétrico

Preparação e caracterização de nanopartículas de fibroína obtidas de casulos de *Bombyx mori* L. Pilamo I

Resumo: A fibroína da seda (SF) é uma biomacromolécula composta de proteínas com propriedades como biocompatibilidade, biodegradabilidade e baixa imunogenicidade. Portanto, as nanopartículas de fibroína da seda (FNps) superam as desvantagens das nanopartículas sintéticas não degradáveis. Nós estudamos as propriedades estruturais e térmicas de SF e FNps derivadas de casulos de *Bombyx mori* L. híbrido Pilamo I. A fibroína crua (RF) foi extraída usando uma solução de sódio Na_2CO_3 como parte de um design experimental para aprimorar a extração. As FNps foram preparadas desnaturando a RF com uma solução ternária de $\text{CaCl}_2:\text{H}_2\text{O}:\text{CH}_3\text{CH}_2\text{OH}$, seguido de precipitação usando um método anti-solvente com propanol. O casulo de Pilamo I, a RF e as FNps foram caracterizados por meio de espectroscopia no infravermelho com transformada de Fourier (FTIR), microscopia eletrônica de varredura (SEM) e análise química elementar de raios X por dispersão em energia (EDS). A dispersão de Luz (DLS) e as propriedades térmicas da RF e as FNps foram estudadas por termogravimetria (TGA) e calorimetria diferencial de barrido (DSC). Os resultados da FTIR mostraram que se obteve fibroína livre de sericina, e os resultados do SEM mostraram que partículas de nanômetros de tamanho tinham estrutura globular e porosidade aparente. As diferenças na entalpia dos picos de cristalização nas curvas de DSC e TGA mostraram que as FNps tinham uma estabilidade térmica maior do que as fibras de RF. Este resultado avança o desenvolvimento de materiais alternativos que possam servir de meio de transporte para compostos ativos de extratos naturais.

Palavras-chave: fibroína, Nanopartículas, FTIR, SEM, Termogravimetria

Gloria Edith Guerrero-Álvarez

Doctor in chemistry, professor of analytical chemistry at the Technological University of Pereira and director of the OLEOQUIMICA research group. Her research area is focused on the use of sericulture products and by-products.

ORCID: 0000-0002-0529-5835

Luz Marina Baena

Industrial Chemistry, candidate for the master's degree in Chemical Sciences at the Technological University of Pereira, researcher of the OLEOQUIMICA research group and professor of organic chemistry. Her research area is focused on the use of sericulture.

ORCID: 0000-0003-0792-9077

Maria Camila Giraldo González

Industrial Chemistry, graduate from the Technological University of Pereira, developed her degree work in the Oleochemical Research Group.

ORCID: 0000-0002-0109-8439